Complex population structure of the Atlantic puffin revealed by whole genome analyses

Oliver Kersten[1]*, Bastiaan Star[1], Deborah M. Leigh[2], Tycho Anker-Nilssen[3], Hallvard Strøm[4], Jóhannis Danielsen[5], Sébastien Descamps[4], Kjell E. Erikstad[4,6], Michelle G. Fitzsimmons[7], Jérôme Fort[8], Erpur S. Hansen[9], Mike P. Harris[10], Martin Irestedt[11], Oddmund Kleven[3], Mark L. Mallory[12], Kjetill S. Jakobsen[1], Sanne Boessenkool[1]*

[1] Centre for Ecological and Evolutionary Synthesis (CEES), Department of Biosciences, University of Oslo, Blindernveien 31, 0371 Oslo, Norway

[2]WSL Swiss Federal Research Institute, Zürcherstrasse 111, 8903 Birmensdorf, Switzerland

[3] Norwegian Institute for Nature Research (NINA), Høgskoleringen 9, NO-7034 Trondheim, Norway

[4] Norwegian Polar Institute, Fram Centre, Postbox 6606, Langnes, 9296 Tromsø, Norway

[5]Faroe Marine Research Institute (FAMRI), Nóatún 1, FO-100 Tórshavn, Faroe Islands

[6]Centre for Biodiversity Dynamics (CBD), Norwegian University of Science and Technology (NTNU), Trondheim, Norway

[7]Environment and Climate Change Canada, Newfoundland and Labrador, Canada

[8]Littoral, Environment et Sociétés (LIENSs), UMR 7266 CNRS – La Rochelle Université, 17000 La Rochelle, France

[9]South Iceland Nature Research Centre, Ægisgata 2, 900 Vestmannaeyjar, Iceland

[10]UK Centre for Ecology & Hydrology, Penicuik, Midlothian, EH26 0QB, UK

[11]Department for Bioinformatics and Genetics, Swedish Museum of Natural History, Box 50007, 104 05 Stockholm, Sweden

[12]Department of Biology, Acadia University, Wolfville, Nova Scotia, Canada, B4P 2R6

**Email: oliver.kersten@ibv.uio.no, sanne.boessenkool@ibv.uio.no*

Abstract

The factors underlying gene flow and genomic population structure in vagile seabirds are notoriously difficult to understand due to their complex ecology with diverse dispersal barriers and extensive periods at sea. Yet, such understanding is vital for conservation management of seabirds that are globally declining at alarming rates. Here, we elucidate the population structure of the Atlantic puffin (*Fratercula arctica*) by assembling its reference genome and analyzing genome-wide resequencing data of 72 individuals from 12 colonies. We identify four large, genetically distinct clusters, observe isolation-by-distance between colonies within these clusters, and obtain evidence for a secondary contact zone. These observations disagree with the current taxonomy, and show that a complex set of contemporary biotic factors impede gene flow over different spatial scales. Our results highlight the power of whole genome data to reveal unexpected population structure in vagile marine seabirds and its value for seabird taxonomy, evolution and conservation.

38 **Main**

39 Seabirds are important ecosystem indicators and drivers[e.g. 1–3], and have long had an integral
40 place in human culture and economy[4–6]. Nevertheless, global seabird numbers have deteriorated
41 by an alarming 70% since halfway of the 20th century[e.g. 7,8]. These declines pose a serious threat
42 to marine ecosystems, human society, and culture[e.g. 7,9,10], highlighting the importance of seabird
43 conservation management. Within such management the identification of distinct population units
44 is a fundamental first step towards optimized conservation[11–13]. Defining such units is, however,
45 difficult for many seabirds because their complex ecology promotes dispersal barriers due to e.g.
46 oceanography, foraging behavior, at-sea range, and phenology[14]. Detailed genomic data
47 including thousands of loci provide new possibilities to assess levels of connectivity and gene flow
48 between distinct breeding populations and, thus, help identify relevant conservation units for
49 seabirds[14,15]. Indeed, a few recent publications using reduced genomic representation
50 approaches (e.g. RAD-seq) report fine-scale structure over various spatial scales[16–20]. These
51 studies highlight the great potential of genomic data to disentangle barriers to gene flow that would
52 otherwise remain undetected, but remain nonetheless limited due to incomplete sampling of the
53 genome[21].

54 The Atlantic puffin (*Fratercula arctica*, Linnaeus, 1789, hereafter “puffin”) is an iconic
55 seabird species, prevalent in popular culture[e.g. 22], important for tourism[e.g. 23,24] and inherently
56 valuable for the marine ecosystem[e.g. 1]. Puffins were historically widely harvested for their meat
57 and down[6,25,26] and exploitation remains an important cultural tradition in Iceland and the Faroe
58 Islands[6,23]. Its breeding range stretches from the Arctic coast and islands of European Russia,
59 Norway, Greenland, and Canada, southward to France and the USA[27] (Figure 1a). Puffins have
60 been designated as "vulnerable" to extinction globally and listed as “endangered” in Europe[28].
61 Notably, the once world’s largest puffin colony (Røst, Norway) has experienced complete fledging
62 failure during nine of the last 13 seasons and has lost nearly 80% of its breeding pairs during the
63 last 40 years[28–30]. Similarly, Icelandic and Faroese puffins have experienced low productivity and

64 negative population growth since 2003[31]. Puffins have been broadly classified into three
65 taxonomic groups along a latitudinal gradient based on size, with the *smallest* puffins found
66 around France, Britain, Ireland and southern Norway (*F. a. grabae*), *intermediate* sized puffins
67 around Norway, Iceland and Canada (*F. a. arctica*) and the *largest* puffins found in the High Arctic,
68 e.g. Spitsbergen, Greenland and northeastern Canada[32] (*F. a. naumanni*)[33] (Figure 1a).
69 Nevertheless, this broad classification into three subspecies has been controversial[27,34,35] and the
70 population structure of puffins remains unresolved at all spatial scales[34]. This knowledge gap
71 obstructs efforts towards an assessment of dispersal barriers, limits our understanding of cause-
72 and-effect dynamics between population trends, ecology and the marine ecosystem, and hinders
73 the development of adapted large-scale conservation actions.

74 Here, we present the first whole genome analysis of structure, gene flow and taxonomy of
75 a pelagic, North Atlantic seabird. We generated a *de novo* draft assembly for the puffin and
76 resequenced 72 individuals across 12 colonies representing the majority of the species' breeding
77 range (Figure 1a). Our work provides compelling evidence that a complex interplay of ecological
78 factors contributes to the range-wide genomic population structure of this vagile seabird.

Results

Genome assembly and population sequencing

Based on synteny with the razorbill (*Alca torda*), a total of 13,328 puffin scaffolds were placed into 26 pseudo-chromosomes, leaving 17.06 Mbp (1.4%) unplaced and yielding an assembly of 1.294 Gbp (Table S1, S2). This assembly contains 4,522 of the 4,915 genes (92.0%) of complete protein coding sequences from the avian set of the OrthoDB v9 database (Table S1). We also assembled the puffin mitogenome (length of 17,084 bp) with a similar arrangement of genomic elements as other members within the bird family Alcidae[36,37] (Figure S1, Table S3). For the 72 resequenced specimens, we analyzed a total of 5.77 billion paired reads, obtaining an average fold-coverage of 7X (range 3.0 - 10) for the nuclear genome and 591X (5.3 - 1800) for the mitochondrial genome per specimen (Figure 1a, Table S4). One individual (IOM001) was removed from the dataset due to a substantially lower number of mapped reads (endogeny) relative to all other samples (Table S4) resulting in a large proportion of missing sites (Figure S2). Additional filtering produced a final genotype likelihood dataset of 1,093,765 polymorphic nuclear sites and 192 mitochondrial single-nucleotide-polymorphisms (SNPs) in 71 birds (36 males and 35 females).

Genomic population structure

Genomic variation across 71 puffin mitogenomes defines 66 polymorphic haplotypes that indicate a recent global population expansion and show no significant population structure (Figure 1b, Figure S3, Table S5, S6). In contrast, we inferred four main population clusters using Principal Component Analysis (PCA) of the nuclear whole-genome dataset (Figure 1c). Puffins from Spitsbergen are most distinct, while puffins from Bjørnøya are located between Spitsbergen and a larger, central cluster consisting of populations from Norway, Iceland and the Faroe Islands (Figure 1c, Figure S4a). Puffins from Canada form their own distinct cluster, as do those from the Isle of May, southeast Scotland (Figure 1c, Figure S4b). Hierarchical PCA analyses of the cluster

comprising the mainland Norwegian, Icelandic and Faroese colonies reveal further fine-scale structure separating Norwegian (Hornøya and Røst) and Faroese/Icelandic colonies (Figure S4c). Model-based clustering (ngsAdmix) agrees with the results from the PCA (Figure 1b). The optimal model fit for the entire dataset is either K = 2 or K = 4 (Figure S5a), as determined by the method of Evanno et al.[38]. At K = 2, ngsAdmix separates Spitsbergen from the other colonies, with Bjørnøya being admixed (following separation along PCA 1), whereas at K = 4, ngsAdmix reflects the structure of three additional distinct clusters representing Spitsbergen, Canada, the Isle of May, and a central group with more shared ancestry. The shared ancestry of the central group remains present in hierarchical admixture analyses excluding Spitsbergen and Bjørnøya individuals (Figure S5b, S6). We find no fixed alleles and pairwise F_{ST} values between colonies and genomic clusters are low (<0.01) (Table S6), apart from any comparisons involving the Spitsbergen population, which show substantially higher F_{ST} values (0.03-0.08).

Phylogenetic reconstructions using individual-based Neighbor-Joining (NJ) and maximum likelihood (ML) methods (Figure 2a, Figure S7), as well as population-based analyses in Treemix (Figure 2b), support the distinctiveness of the Spitsbergen, Canada and the Isle of May puffins with each group forming monophyletic clades with 100% bootstrap support. In contrast, Bjørnøya forms a paraphyletic clade between Spitsbergen and northern Norway (Figure 2a). The population clusters identified by the PCA and ngsAdmix at smaller spatial scales are also identified in the topologies of the NJ and ML trees, sorting individuals predominantly according to geographical location, although with low bootstrap support (> 80) due to large inter-individual variability (Figure 2a, S6). Allowing a single migration edge in the Treemix phylogeny identifies recent gene flow from Spitsbergen to Bjørnøya (likelihood = 792.106; Figure S8, S9a). Adding additional migration edges to the population-based ML tree does not improve the model fit and such edges are therefore not further interpreted (Figure S8-S10).

Genetic diversity, heterozygosity and inbreeding

131 Tajima's D does not significantly deviate from neutral expectation per colony (Table S5).
132 Nucleotide diversity (π) of puffins is significantly different between colonies, with the Spitsbergen
133 population having significantly lower nucleotide diversity than the global median (Wilcoxon Rank
134 Sum test, $U = 4824$, $n_{SPI} = 25$, $n_{Global} = 300$, $p < 0.05$, Table S5). Colonies also differ significantly
135 in levels of heterozygosity (Kruskal-Wallis Test, $p < 0.001$; Figure 3a) and inbreeding (Kruskal-
136 Wallis Test, $p < 0.001$, Figure 3b), whereby individual inbreeding (F_{RoH}) was approximated based
137 on Runs of Homozygosity (RoH)[39]. Again, the Spitsbergen colony has significantly lower levels of
138 heterozygosity (0.00220 - 0.00223) and significantly higher levels of F_{RoH} values (0.161 - 0.172),
139 compared to the Faroese and Icelandic colonies (Dunn test with Holm correction, $p < 0.05$). The
140 Faroese and Icelandic colonies contain the highest levels of heterozygosity and lowest F_{RoH}
141 values (Figure 3a, 3b, S11) overall. The remaining colonies display intermediate levels (Figure
142 3a, 3b), although heterozygosity is significantly lower (Figure 3a, S11) and inbreeding is
143 significantly higher (Figure 3b, S11) on Gull Island and Bjørnøya compared to the Icelandic and
144 Faroese colonies (Dunn test with Holm correction, $p < 0.05$). Moreover, Spitsbergen harbors the
145 most (an average of 718 per individual) and longest RoHs with eight being ≥ 2.3 Mbp long (4.21
146 ± 3.02 % of respective chromosome), whereas none of the RoHs in the remaining colonies were
147 > 2.15 Mbp long (Figure 3c). The only exception was a 9.65 Mbp long RoH on pseudo-
148 chromosome 7 (18% of chromosome length) in an Isle of May individual (Figure 3c).
149
150 *Patterns of gene flow and Isolation-By-Distance (IBD)*
151 We investigated patterns of gene flow and IBD between the colonies using two-dimensional
152 estimated effective migration surface (EEMS) analyses. Levels of gene flow between the Icelandic
153 and Faroese colonies and within the Canadian group is high (3-10x higher than the global
154 average), while intermediate between the Norwegian mainland colonies (around the global
155 average). In contrast, the Spitsbergen colony is split from the remaining colonies by migration
156 rates up to 100x lower than the global average (Figure 4a, S12), while additional regions of low

157 gene flow (2-3x lower than the global average) separate the Isle of May, Canadian, and Bjørnøya
158 colonies from the rest (Figure 4a, Figure S12). Geographic distance between all puffin colonies
159 is a poor predictor of pairwise genetic distance, driven by the high Slatkin's linearized F_{ST} values
160 of the Spitsbergen colony (Figure S13). Nevertheless, geographic distance among a subset of
161 puffin colonies is significantly correlated with genetic distance using Mantel tests (Figure 4b, S13).
162 Specifically, by progressively removing the more distant colonies (Spitsbergen, Bjørnøya, Isle of
163 May, Canada), the fit of a linear IBD model is significantly improved and the proportion of genetic
164 dissimilarity explained by geographic distance is more than doubled (No SPI = 38.16 %,
165 SPI/BJO/IOM removed = 79.77 %) (Figure 4b, S13). The isolated colonies are characterized by
166 high Slatkin's linearized F_{ST} values at relatively small geographic distances (Figure S13).
167
168 *Admixture on Bjørnøya*
169 We specifically tested for patterns of admixture in Bjørnøya. Significantly negative $f3$ statistics (Z
170 score < -3) are found for all unique combinations of the phylogeny (Spitsbergen, *X*; Bjørnøya)
171 (Table S7), indicating an admixed colony on Bjørnøya caused by gene flow between Spitsbergen
172 and the remaining colonies. Similarly, significantly positive D-statistics (Z score > 3) caused by
173 an excess of ABBA sites reveal excessive allele sharing between Spitsbergen and Bjørnøya
174 (Figure S14a). The close association and gene flow from Spitsbergen to Bjørnøya is further
175 confirmed by D-statistics not being significantly different from 0 for the (((Bjørnøya, Spitsbergen),
176 H3), Razorbill) topology (Figure S14b).

Discussion

Barriers to gene flow leading to population structure are notoriously difficult to identify and remain largely unknown for most seabirds[14,40]. Using whole genome analyses, we here provide novel insights into the genetic structure of the Atlantic puffin. First, we identify four main puffin population clusters consisting of (1) Spitsbergen (High Arctic), (2) Canada, (3) Isle of May, and (4) multiple colonies in Iceland, the Faroe Islands and Norway. Second, we find that *within* such clusters, genetic differentiation is driven by isolation-by-distance (IBD). Finally, we find evidence for secondary contact between two clusters. These observations show that a complex set of drivers impacts gene flow over different spatial scales (100s -1000s of km) between these clusters and the colonies within. In particular, the interplay between overwintering grounds, philopatry, natal dispersal, geographic distance, and potentially ocean regimes appears to explain the genomic differentiation between puffin colonies.

Mature puffins rarely, if ever, change their colonies, resulting in very high colony fidelity once they start breeding[27]. Immatures, however, have been observed to visit other nearby colonies during the summer and may breed in non-natal colonies[27,41]. Nevertheless, data on natal philopatry remain scarce, but existing evidence shows rates vary greatly (38-92%) between colonies[27,41]. If either breeding or natal philopatry alone drive the puffin population structure, each colony should constitute its own distinct genomic entity and significant relationships between geographic and genomic distance across the puffin's entire breeding range would be observed. Yet, philopatry alone cannot explain the presence of the four large-scale population clusters we observe here. Additional factors must therefore promote the distinctiveness of the four clusters. For instance, the Isle of May birds have a largely separate overwintering distribution mainly in the North Sea (Figure S15)[27,35,42]. Such potential geographical separation during the winter season might limit the likelihood of immatures intermixing between the Isle of May and other colonies. Similarly, distinct overwintering distributions have been found to lead to increased genetic diversification in other philopatric seabird species[14,40,43], such as the thick-billed murre (*Uria*

203 *lomvia*)[20] and black-browed albatross (*Thalassarche melanophris*)[44]. The presence of a Canadian
204 cluster can also be largely explained by their winter distribution around Newfoundland[42,45]. There
205 is, however, some fragmentary overlap in the overwintering distribution of the Canadian and
206 Icelandic colonies off southwestern Greenland[42,45], suggesting that barriers to migration of
207 immatures and gene flow in the western Atlantic may be further enforced by the large geographic
208 distance. In contrast, the winter distribution from the colonies in Iceland, Norway and the Faroe
209 Islands overlaps off the coast of southern Greenland (Figure S15)[42]. This shared overwintering
210 area, combined with the tendency to return to the natal colony and immature visits of nearby (up
211 to 100s km) colonies during the summer, appears to drive a pattern of IBD among colonies (Figure
212 3b). Indeed, IBD has previously been recognized as an important driver of genomic structure in
213 seabirds, for instance in the little auk (*Alle alle*)[46] and band-rumped storm-petrel (*Oceanodroma*
214 *castro*)[47]. While these illustrated mechanisms provide reasonable explanations for the observed
215 dispersal barriers and population structure based on our current knowledge, validation requires
216 additional evidence, specifically on the winter distribution of immature puffins and natal emigration
217 rates across colonies covering the entirety of the puffin's breeding range.

218 High Arctic puffins from Spitsbergen are genetically the most divergent group within our
219 dataset. They are also characterized by significantly lower levels of genetic diversity, greater
220 inbreeding coefficients, and longer and more abundant RoHs compared to other colonies. These
221 observations may either result from a historical bottleneck followed by isolation (e.g. founder
222 effect), local adaptation to their extreme environment or generally lower effective population sizes.
223 Population abundance estimates of less than 10,000 breeding pairs on Spitsbergen compared to
224 500,000 in the West Atlantic, two million on Iceland and more than two million in the boreal East
225 Atlantic potentially indicate a lower effective population size[27]. The High Arctic puffins exclusively
226 inhabit harsh, cold-current environments, also in the winter, during which they likely stay in an
227 area bounded by the East Greenland ice edge, a latitudinal border at 70° N and the front between
228 the Barents and Greenland Sea (Figure S15). They are also substantially larger than birds from

229 lower latitudes[27], following Bergmann's[48] or James's[49] rule, as has been observed in other
230 seabirds[e.g. 50,51]. This matches the clinal size variation of puffins that closely tracks sea
231 temperatures in their breeding areas[52]. Despite these distinctions, we find that the relatively small
232 population of puffins on Bjørnøya (< 1,000 pairs[27]), midway between Spitsbergen and mainland
233 Norway, represents an area of secondary contact between the puffins from the High Arctic and
234 other puffin colonies. Based on D- and the $f3$-statistics, the most likely southern sources are
235 Iceland, the Faroe Islands, Norway, or a combination thereof. Thus, the barriers to gene flow that
236 keep the Spitsbergen colonies distinct do not prevent formation of a hybrid colony where
237 individuals from the High Arctic and the cluster composed of mainland Norwegian, Icelandic and
238 Faroese colonies meet.

239 The distinct population structure in the nuclear data is not observed in the mitochondrial
240 genomes, which reveal an abundance of rare alleles and lack of significant population
241 differentiation. The mitogenomic variation suggests that puffins experienced a recent population
242 expansion, possibly out of a refugium after the Last Glacial Maximum. Indeed, it has been shown
243 that mitogenomic variation in seabirds is dominated by historical factors rather than representing
244 contemporary gene flow[40], and a lack of mitogenomic population structure has been observed in
245 many marine birds with high philopatry[e.g. 46,53,54]. In contrast to the mitogenomes, the structure in
246 the nuclear data therefore likely originated after the last glacial period and reflects the influence
247 of relatively recent barriers to gene flow in a context of historical demography[14,40]. Such results
248 are relevant for understanding the "seabird paradox", which contrasts the life-history traits of high
249 philopatry and restricted dispersal in otherwise highly mobile species[55].

250 Our results have major implications for the conservation management of the Atlantic
251 puffin. The genetic structure we identify in puffins disagrees with the suggestion of three
252 subspecies (*F. a. naumanni, F. a. arctica, F. a. grabae*)[33]. Although the genetically distinct
253 Spitsbergen cluster coincides with the classification of morphologically large puffins in the High
254 Arctic (*F. a. naumanni*)[27], we observe gene flow from Spitsbergen into Bjørnøya, which has been

255 considered *F. a. arctica*[27]. Furthermore, the geographic divide between *F. a. grabae* and *F. a.*
256 *arctica* lies farther south than previously thought, with the Faroese puffins being genetically closer
257 to *F. a. arctica* than to *F. a. grabae*. Nonetheless, *F. a. grabae* is currently represented by a single
258 colony (Isle of May) in our study and the geographical extent of this genomic cluster needs to be
259 refined by additional sampling, particularly in the western UK, Ireland, and France. Finally, puffins
260 from the Western Atlantic region (e.g. colonies in Canada) form their own distinct genetic cluster
261 that is not recognized within the current classification. Our results do not only warrant a revision
262 of Salomonsen's taxonomic classification of three subspecies[33], but also highlight the need to
263 acknowledge the four identified clusters as distinct units within the conservation management of
264 puffins[11–13]. Although puffin colonies *within* clusters are not genetically distinct entities, ecological
265 independence illustrated by contrasting population dynamics across relatively small spatial scales
266 (e.g. western Norway[30]) suggests that higher resolution local management units based on
267 ecological differences should be considered. Nonetheless, the observation that the genetically
268 distinct clusters are at the outer edges of the puffin's distribution, indicates that the management
269 and conservation of these distinct clusters must be a priority. Finally, our sampling does not cover
270 several outskirts of the puffin's distribution, such as the US, northern Canada, Greenland, Ireland,
271 western UK, France or Russia, and we may therefore still underestimate the true biological and
272 genetic complexity of this species.

273 In conclusion, our study shows that a complex interplay of barriers to gene flow drives a
274 previously unrecognized population diversification in the iconic Atlantic puffin. So far, much of
275 seabird population genetics research has been based on mitochondrial and microsatellite
276 data[14,40], which have limited power to characterize contemporary factors that determine
277 population structure and gene flow[19,56]. High-resolution nuclear data are therefore essential to
278 help define evolutionary significant population units, disentangle convoluted ecological
279 relationships, and are particularly important for seabird conservation, which aims to preserve

genetic diversity considering profound global population declines[e.g. 7,8] and the threat of global warming, which negatively impacts ecosystems worldwide[57].

282 **Methods**

283

284 *Draft reference genome assembly*

285 A *de novo* Atlantic puffin draft genome was generated from the blood of a female Atlantic puffin.
286 Read data was sequenced on three Illumina HiSeqX lanes using the 10x Genomics Chromium
287 technology and assembled with the Supernova assembler (v2.1.1)[58] after subsampling to 0.8
288 billion and 1 billion reads to maximize performance and remain within the computational capacity
289 of the assembler. We refined the two assemblies through several steps, including merging of
290 'haplotigs', removal of contaminant sequences, misassembly correction, re-scaffolding using
291 mapping coverage and linkage information, and gap filling (Table S1a). The most complete and
292 continuous 800M and 1000M assemblies together with the 3rd best assembly overall were
293 selected for a second round of refinement (Table S1b) resulting in a total of 72 draft assemblies.
294 Of these, we kept the four most complete and continuous assemblies for additional gap filling and
295 polishing, after which the most complete draft genome was selected for downstream analyses
296 (Table S1c). The puffin mitogenome was confidently identified by blasting (blastn) all scaffolds
297 shorter than 25 kb against a custom-built database of 135 published mitogenomes of the order
298 'Charadriiformes' and annotated with the MITOS web server[59] (Figure S1). The remaining nuclear
299 scaffolds were ordered and concatenated into "pseudo-chromosomes" by mapping them to the
300 razorbill genome (*Alca torda* - NCBI: bAlcTor1 primary, GCA_008658365.1) and applying 200 N's
301 as padding between each scaffold. We combined unmapped scaffolds into an "unplaced" pseudo-
302 chromosome. We assessed order and placement of scaffolds by investigating synteny in
303 coverage and length between the puffin and razorbill chromosomes (Table S2). Details on the
304 draft reference genome assembly and refinement can be found in the Supplementary File.

305

306 *DNA extraction and sequencing*

307 Samples from a total of 72 puffins collected across 12 breeding colonies (Figure 1a) were made
308 available for the present study by SEAPOP (http://www.seapop.no/en), SEATRACK
309 (http://www.seapop.no/en/seatrack) and ARCTOX (http://www.arctox.cnrs.fr/en/home - Canadian
310 colonies). These samples had been collected between 2012-2018 and consisted of blood
311 preserved in EtOH or lysis buffer, or feathers (Table S4). We extracted DNA using the DNeasy
312 Blood & Tissue kit (Qiagen) following the manufacturer's protocol for animal blood or the
313 nail/hair/feathers protocol applying several modifications for improved lysis and DNA yield.
314 Individuals that had no sexing data associated with them were sexed using PCR amplification of
315 specific allosome loci and visualization via gel electrophoresis. Genomic libraries were built by
316 the Norwegian Sequencing Centre and sequenced on an Illumina HiSeq4000. We processed
317 sequencing reads in PALEOMIX v1.2.14[60] and split the resulting bam files into nuclear and
318 mitochondrial bam files. Additional details on the DNA extraction, sexing, sequencing and
319 mapping are listed in the Supplementary File.
320
321 *Mitogenome analyses*
322 Genotypes across the mitochondrial genome were jointly called with GATK v4.1.4[61] by using the
323 *HaplotypeCaller*, *CombineGVCFs* and *GenotypeGVCFs* tool. We filtered genotypes according to
324 GATKs Best Practices[62] and set genotypes with a read depth less than 3 or a quality less than 15
325 as missing. Indels and non-biallelic SNPs were removed and only SNPs present in all individuals
326 were kept for subsequent analyses. The SNP dataset was annotated with snpEff[63] utilizing the
327 annotation of the newly assembled mitogenome of the Atlantic puffin and converted into a
328 mitogenome sequence alignment. To serve as an outgroup, we appended four other species of
329 the family Alcidae, i.e. the Razorbill (*Alca torda*, NCBI: CM018102.1), the Crested Auklet (*Aethia*
330 *cristatella*, NCBI: NC_045517.1), the Ancient Murrelet (*Synthliboramphus antiquus*, NCBI:
331 NC_007978.1) and the Japanese Murrelet (*Synthliboramphus wumizusume*, NCBI:
332 NC_029328.1), to the alignment. To construct a maximum-likelihood phylogenetic tree, we split

333 the alignment into seven partitions, i.e. one partition for a concatenated alignment of each of the
334 three codon positions of the protein coding genes, one partition for the concatenated alignment
335 of the rRNA regions, one partition for the concatenated alignment of the tRNAs, one partition for
336 the alignment of the control region, and one partition for the concatenated alignment of the
337 "intergenic" regions. The best-fitting evolutionary model for each partition was found by
338 *ModelFinder*[64] and the tree was built with IQTree v1.6.12[65] using 1000 ultrafast bootstrap
339 replicates. We used the resulting tree to draw a haplotype genealogy graph with Fitchi[66]. Using
340 Arlequin v.3.5[67], we calculated haplotype (h), nucleotide diversity (π) and Tajima's D[68] for each
341 colony, for each genomic cluster defined by the nuclear analysis, and globally. Additionally, an
342 Ewens–Watterson test[69], Chakraborty's test of population amalgamation[70] and Fu's F_s test[71] were
343 conducted for each of those groups. To further identify population differentiation, the proportion
344 of sequence variation (Φ_{ST}) was estimated for all pairs of populations and genomic clusters.
345 Hierarchical AMOVA tests subsequently determined the significance of *a priori* subdivisions into
346 colonies and genomic clusters. Calculation of Φ_{ST} and AMOVA tests were also conducted in
347 Arlequin. Additional details on the mitochondrial analyses are given in the Supplementary File.
348
349 *Nuclear genome clustering and phylogenetic analyses*
350 The majority of population genomic analyses were based on nuclear genotype likelihoods as
351 implemented in ANGSD v.0.931[72]. After assessing the quality of the mapped sequencing data in
352 an ANGSD pre-run, we removed an individual from the Isle of May from the dataset. Genotype
353 likelihoods for nuclear SNPs covered in all individuals were calculated and filtered in ANGSD.
354 Accounting for linkage disequilibrium, we further pruned the dataset by only selecting the most
355 central site within blocks of linked sites (r^2>0.2) as in Orlando and Librado (2019)[73]. Subsequently,
356 all variants located on the Z-pseudo-chromosome and "unplaced scaffolds" were excluded from
357 the analyses yielding a final genotype likelihood panel consisting of 1,093,765 sites. We
358 investigated genomic population structure with a Principal Component Analysis (PCA) of the

359 genotype likelihood panel using PCAngsd v0.982[74] and estimated individual ancestry proportions
360 using a maximum likelihood (ML) approach implemented in ngsAdmix v32[75], with the number of
361 ancestral populations (K) set from 1 to 10. Additional "hierarchical" PCA and admixture analyses
362 were conducted for genomic sub-cluster(s) using identical methods.

363 After adding the razorbill genome as an outgroup to the genotype likelihood panel by
364 mapping unpublished, raw 10x Genomics sequencing data used for the assembly of the
365 embargoed razorbill genome to the puffin draft assembly, we built a neighbor-joining (NJ) tree
366 based on pairwise genetic distance matrices (p-distance) and a sample-based ML phylogenetic
367 tree in FastMe v2.1.5[76] and Treemix v1.13[77], respectively. For both trees, 100 bootstrap replicates
368 were generated. To infer patterns of population splitting and mixing, we produced population-
369 based ML trees including up to ten migration edges. The optimal number of migrations was
370 selected using a quantitative approach by evaluating the distribution of explained variance, the
371 log likelihoods, the covariance with an increase in migration edges, and by applying the method
372 of Evanno[38] and several different linear threshold models. The topology for m_0 and m_{BEST} was
373 evaluated by generating 100 bootstrap replicates. Additional details on the cluster and
374 phylogenetic analyses are given in the Supplementary File.

375

376 *Genetic diversity, heterozygosity and inbreeding*

377 We calculated a set of neutrality tests and population statistics in ANGSD using colony-based
378 one-dimensional (1D) folded Site-Frequency-Spectra (SFS). For each population, genomic
379 cluster, and globally, Tajima's D and nucleotide diversity (π) were computed utilizing the per-site
380 θ estimates. Individual genome-wide heterozygosity was calculated in ANGSD using individual,
381 folded, 1D SFS. We calculated heterozygosity by dividing the number of polymorphic sites by the
382 number of total sites present in the SFS.

383 The proportion of runs of homozygosity (RoH) within each puffin genome was computed
384 by calculating local estimates of heterozygosity in 100 kbp sliding windows (50 kbp slide) following

385 the approach in Sánchez-Barreiro et al. (2020)[39]. We defined the 10% quantile of the average
386 local heterozygosity across all samples as the cutoff for a “low heterozygosity region”. RoHs were
387 declared as all regions with at least two subsequent windows of low heterozygosity (below cutoff)
388 and their final length was calculated as described in Sánchez-Barreiro et al. (2020)[39]. We
389 calculated an individual inbreeding coefficient based on the RoH, F_{RoH} , as in Sánchez-Barreiro
390 et al. (2020)[39] by computing the fraction of the entire genome falling into RoHs, with the entire
391 genome being the total length of windows scanned. Additional details on these analyses can be
392 found in the Supplementary File.
393
394 *Patterns of gene flow and admixture*
395 Assessing potential landscape genetic patterns of IBD within the breeding range of the puffin, the
396 program EEMS[78] was used to model the association between genetic and geographic data by
397 visualizing the existing population structure and highlighting regions of higher-than-average and
398 lower-than-average historic gene flow. We calculated a pairwise genetic distance matrix in
399 ANGSD by sampling the consensus base (*-doIBS 2 -makeMatrix 1*) at the sites included in the
400 genotype likelihood set (see *Nuclear cluster and phylogenetic analyses*) for each sample. The
401 matrix was fed into 10 independent runs of EEMS, each consisting of one MCMC chain of six
402 million iterations with a two million iteration burn-in, 9999 thinning iterations, and 1000 underlying
403 demes. Supplementing the results of the EEMS analysis, we conducted a traditional IBD analysis
404 by determining geographical and genetic distances between the 12 colonies and assessing the
405 significance of the correlation between the two distance matrices with a Mantel test[79] and a
406 Multiple Regression on distance Matrix (MRM)[80] analysis. F_{ST} was used as a proxy for genetic
407 distance and computed for each population pair in ANGSD by applying two-dimensional (2D),
408 folded SFS. We converted pairwise F_{ST} values to Slatkin’s linearized F_{ST}[81]. Great circle distances
409 between colony coordinates (latitude/longitude) were calculated using the R package marmap[82]
410 and used as geographic distances. We performed the Mantel test (10,000 permutations) and

411 MRM analysis with the R package *ecodist*[83]. All analyses for IBD were re-run on subsets of
412 colonies by progressively removing the Spitsbergen, Bjørnøya, Isle of May, and Canadian
413 colonies from the geographic and genetic distance matrices.

414 Additional assessments of gene flow and admixture were conducted by calculating f3-
415 statistics and multi-population D-statistics (aka ABBA BABA test)[84]. We calculated f3-statistics in
416 Treemix for each unique combination of ((A,B),C)) of the 12 puffin populations. D-statistics were
417 calculated in ANGSD (-doAbbababa2) for each combination of ((A,B),C),Outgroup) using the 12
418 puffin colonies. The outgroup was generated in ANGSD using the 10xGenomics sequencing data
419 of the razorbill mapped to the puffin reference genome (see *Nuclear cluster and phylogenetic*
420 *analyses)*. Additional details on the IBD and admixture analyses are given in the Supplementary
421 File.
422

423 **References**
424

425 1. Otero, X. L., De La Peña-Lastra, S., Pérez-Alberti, A., Ferreira, T. O. & Huerta-Diaz, M. A.
426 Seabird colonies as important global drivers in the nitrogen and phosphorus cycles. *Nat.*
427 *Commun.* **9**, 246 (2018).
428 2. Velarde, E., Anderson, D. W. & Ezcurra, E. Seabird clues to ecosystem health. *Science*
429 **365**, 116–117 (2019).
430 3. Piatt, J. F., Sydeman, W. J. & Wiese, F. Introduction: a modern role for seabirds as
431 indicators. *Mar. Ecol. Prog. Ser.* **352**, 199–204 (2007).
432 4. Boersma, P. D., Clark, J. A. & Hillgarth, N. Seabird conservation. in *Biology of Marine Birds*
433 (eds. Schreiber, E. & Burger, J.) 559–579 (CRC Press Boca Raton, Florida, 2002).
434 5. Denlinger, L. & Wohl, K. Seabird harvest regimes in the circumpolar nations. *Conservation*
435 *of Arctic Flora and Fauna (CAFF)* (2001).
436 6. Merkel, F. & Barry, T. Seabird harvest in the Arctic. *Conservation of Arctic Flora and Fauna*
437 *(CAFF)* (2008).
438 7. Croxall, J. P. *et al.* Seabird conservation status, threats and priority actions: a global
439 assessment. *Bird Conserv. Int.* **22**, 1–34 (2012).
440 8. Paleczny, M., Hammill, E., Karpouzi, V. & Pauly, D. Population trend of the world's
441 monitored seabirds, 1950-2010. *PLoS One* **10**, e0129342 (2015).
442 9. Frederiksen, M. Seabirds in the North East Atlantic. Summary of status, trends and
443 anthropogenic impact. *TemaNord* **587**, 21–24 (2010).
444 10. Chardine, J. & Mendenhall, V. Human disturbance at Arctic seabird colonies. *Conservation*
445 *of Arctic Flora and Fauna (CAFF)* (1998).
446 11. Allendorf, F. W., Hohenlohe, P. A. & Luikart, G. Genomics and the future of conservation
447 genetics. *Nat. Rev. Genet.* **11**, 697 (2010).
448 12. Fraser, D. J. & Bernatchez, L. Adaptive evolutionary conservation: towards a unified

449 concept for defining conservation units. *Mol. Ecol.* **10**, 2741–2752 (2001).
450 13. Funk, W. C., McKay, J. K., Hohenlohe, P. A. & Allendorf, F. W. Harnessing genomics for
451 delineating conservation units. *Trends Ecol. Evol.* **27**, 489–496 (2012).
452 14. Friesen, V. L. Speciation in seabirds: why are there so many species… and why aren't
453 there more? *J. Ornithol.* **156**, 27–39 (2015).
454 15. Taylor, R. S. *et al.* Sympatric population divergence within a highly pelagic seabird species
455 complex (*Hydrobates spp.*). *J. Avian Biol.* **49**, (2018).
456 16. Rexer-Huber, K. *et al.* Genomics detects population structure within and between ocean
457 basins in a circumpolar seabird: The white-chinned petrel. *Mol. Ecol.* **28**, 4552–4572
458 (2019).
459 17. Clucas, G. V. *et al.* Comparative population genomics reveals key barriers to dispersal in
460 Southern Ocean penguins. *Mol. Ecol.* **27**, 4680–4697 (2018).
461 18. Frugone, M. J. *et al.* More than the eye can see: Genomic insights into the drivers of
462 genetic differentiation in Royal/Macaroni penguins across the Southern Ocean. *Mol.*
463 *Phylogenet. Evol.* **139,** (2019).
464 19. Cristofari, R. *et al.* Unexpected population fragmentation in an endangered seabird: the
465 case of the Peruvian diving-petrel. *Sci. Rep.* **9**, 2021 (2019).
466 20. Tigano, A., Shultz, A. J., Edwards, S. V., Robertson, G. J. & Friesen, V. L. Outlier analyses
467 to test for local adaptation to breeding grounds in a migratory arctic seabird. *Ecol. Evol.* **7**,
468 2370–2381 (2017).
469 21. Lowry, D. B. *et al.* Breaking RAD: an evaluation of the utility of restriction site-associated
470 DNA sequencing for genome scans of adaptation. *Mol. Ecol. Resour.* **17**, 142–152 (2017).
471 22. Somvichian-Clausen, A. Behind the stunning photo of a puffin gorging on fish. *National*
472 *Geographic* (2017).
473 23. Huijbens, E. H. & Einarsson, N. Feasting on friends: Whales, puffins, and tourism in
474 Iceland. in *Tourism Experiences and Animal Consumption* 10–27 (Routledge, 2018).

24. Lund, K. A., Kjartansdóttir, K. & Loftsdóttir, K. ‘Puffin love’: Performing and creating Arctic landscapes in Iceland through souvenirs. *Tourist Studies* **18**, 142–158 (2018).
25. Hodgetts, L. M. Animal bones and human society in the late younger stone age of arctic Norway. (Durham University, 1999).
26. Dove, C. J. & Wickler, S. Identification of bird species used to make a Viking age feather pillow. *Arctic* **69**, 29–36 (2016).
27. Harris, M. P. & Wanless, S. *The puffin*. (T & AD Poyser, Bloomsbury Publishing, 2011).
28. BirdLife International. Fratercula arctica. *The IUCN Red List of Threatened Species 2017* (2017)
29. Anker-Nilssen, T. & Aarvak, T. The population ecology of puffins at Røst. Status after the breeding season 2001. *NINA Oppdragsmelding* **736**, 1–40 (2002).
30. Anker-Nilssen, T. *et al.* Key-site monitoring in Norway 2019, including Svalbard and Jan Mayen. *SEAPOP Short Report 1-2020* (2020).
31. Lilliendahl, K. *et al.* Recruitment failure of Atlantic puffins *Fratercula arctica* and sandeels *Ammodytes marinus* in Vestmannaeyjar Islands. *Náttúrufræðingurinn* **83**, 65–79 (2013).
32. Gaston, A. J. & Provencher, J. F. A Specimen of the High Arctic Subspecies of Atlantic Puffin, *Fratercula arctica naumanni*, in Canada. *Can. Field-Nat.* **126**, 50–54 (2012).
33. Salomonsen, F. *The Atlantic Alcidae*. vol. 6 (Elanders boktryckeri aktiebolag, 1944).
34. Moen, S. M. Morphologic and genetic variation among breeding colonies of the Atlantic puffin (*Fratercula arctica*). *Auk* **108**, 755–763 (1991).
35. Harris, M. P. Measurements and weights of British Puffins. *Bird Study* **26**, 179–186 (1979).
36. Kim, J. A., Kang, S.-G., Yang, J. W., Hur, W.-H. & Kil, H.-J. Complete mitochondrial genome of *Aethia cristatella* (Charadriiformes: Alcidae). *Mitochondrial DNA Part B* **5**, 31–32 (2020).
37. Eo, S. H. & An, J. The complete mitochondrial genome sequence of Japanese murrelet (Aves: Alcidae) and its phylogenetic position in Charadriiformes. *Mitochondrial DNA A DNA*

Mapp Seq Anal **27**, 4574–4575 (2016).

38. Evanno, G., Regnaut, S. & Goudet, J. Detecting the number of clusters of individuals using the software STRUCTURE: a simulation study. *Mol. Ecol.* **14**, 2611–2620 (2005).
39. Sánchez-Barreiro, F. *et al.* Historical population declines prompted significant genomic erosion in the northern and southern white rhinoceros (*Ceratotherium simum*). *bioRxiv* (2020) doi:10.1101/2020.05.10.086686.
40. Lombal, A. J., O'dwyer, J. E., Friesen, V., Woehler, E. J. & Burridge, C. P. Identifying mechanisms of genetic differentiation among populations in vagile species: historical factors dominate genetic differentiation in seabirds. *Biol. Rev. Camb. Philos. Soc.* **95**, 625–651 (2020).
41. Breton, A. R., Diamond, A. W. & Kress, S. W. Encounter, survival, and movement probabilities from an Atlantic puffin (*Fratercula arctica*) metapopulation. *Ecological Monographs* **75**, (2006).
42. Fayet, A. L. *et al.* Ocean-wide drivers of migration strategies and their influence on population breeding performance in a declining seabird. *Curr. Biol.* **27**, 3871–3878 (2017).
43. Friesen, V. L., Burg, T. M. & McCoy, K. D. Mechanisms of population differentiation in seabirds. *Mol. Ecol.* **16**, 1765–1785 (2007).
44. Burg, T. M. & Croxall, J. P. Global relationships amongst black-browed and grey-headed albatrosses: analysis of population structure using mitochondrial DNA and microsatellites. *Mol. Ecol.* **10**, 2647–2660 (2001).
45. Lowther, P. E., Diamond, T., Kress, S. W., Robertson, G. J. & Gill, F. Atlantic Puffin (*Fratercula arctica*). *The Birds of North America Online* **18**, (2002).
46. Wojczulanis-Jakubas, K. *et al.* Weak population genetic differentiation in the most numerous Arctic seabird, the little auk. *Polar Biol.* **37**, 621–630 (2014).
47. Smith, A. L., Monteiro, L., Hasegawa, O. & Friesen, V. L. Global phylogeography of the band-rumped storm-petrel (*Oceanodroma castro*; Procellariiformes: Hydrobatidae). *Mol.*

527 *Phylogenet. Evol.* **43**, 755–773 (2007).
528 48. Bergmann, C. Über die Verhältnisse der Wärmeökonomie der Tiere zu ihrer Grösse.
529 *Gottinger Studien* **3**, 595–708 (1847).
530 49. James, F. C. Geographic size variation in birds and its relationship to climate. *Ecology* **51**,
531 365–390 (1970).
532 50. Yamamoto, T. *et al.* Geographical variation in body size of a pelagic seabird, the streaked
533 shearwater *Calonectris leucomelas*. *J. Biogeogr.* **43**, 801–808 (2016).
534 51. Barrett, R. T., Anker-Nilssen, T. & Krasnov, Y. V. Can Norwegian and Russian razorbills
535 (*Alca torda*) be identified by their measurements? *Mar. Ornithol.* **25**, 5–8 (1997).
536 52. Anker-Nilssen, T., Aarvak, T. & Bangjord, G. Mass mortality of Atlantic Puffins *Fratercula*
537 *arctica* off Central Norway, spring 2002: causes and consequences. *Atl. Seabirds* **5**, 57–72
538 (2003).
539 53. Pearce, R. L. *et al.* Mitochondrial DNA suggests high gene flow in ancient murrelets.
540 *Condor* **104**, 84–91 (2002).
541 54. Thomas, J. E. *et al.* Demographic reconstruction from ancient DNA supports rapid
542 extinction of the great auk. *eLife* **8**, (2019).
543 55. Milot, E., Weimerskirch, H. & Bernatchez, L. The seabird paradox: dispersal, genetic
544 structure and population dynamics in a highly mobile, but philopatric albatross species. *Mol.*
545 *Ecol.* **17**, 1658–1673 (2008).
546 56. Edwards, S. & Bensch, S. Looking forwards or looking backwards in avian
547 phylogeography? A comment on Zink and Barrowclough 2008. *Mol. Ecol.* **18,** 2930–2936
548 (2009).
549 57. IPCC. *Global Warming of 1.5 °C - Summary for Policy Makers*. (2018).
550 58. Weisenfeld, N. I., Kumar, V., Shah, P., Church, D. M. & Jaffe, D. B. Direct determination of
551 diploid genome sequences. *Genome Res.* **27**, 757–767 (2017).
552 59. Bernt, M. *et al.* MITOS: improved de novo metazoan mitochondrial genome annotation.

553 *Mol. Phylogenet. Evol.* **69**, 313–319 (2013).
554 60. Schubert, M. *et al.* Characterization of ancient and modern genomes by SNP detection and
555 phylogenomic and metagenomic analysis using PALEOMIX. *Nat. Protoc.* **9**, 1056–1082
556 (2014).
557 61. McKenna, A. *et al.* The Genome Analysis Toolkit: a MapReduce framework for analyzing
558 next-generation DNA sequencing data. *Genome Res.* **20**, 1297–1303 (2010).
559 62. Van der Auwera, G. A. *et al.* From FastQ data to high confidence variant calls: the Genome
560 Analysis Toolkit best practices pipeline. *Curr. Protoc. Bioinformatics* **43**, 11.10.1–33 (2013).
561 63. Cingolani, P. *et al.* A program for annotating and predicting the effects of single nucleotide
562 polymorphisms, SnpEff: SNPs in the genome of *Drosophila melanogaster* strain w1118;
563 iso-2; iso-3. *Fly* **6**, 80–92 (2012).
564 64. Kalyaanamoorthy, S., Minh, B. Q., Wong, T. K. F., von Haeseler, A. & Jermiin, L. S.
565 ModelFinder: fast model selection for accurate phylogenetic estimates. *Nat. Methods* **14**,
566 587–589 (2017).
567 65. Nguyen, L.-T., Schmidt, H. A., von Haeseler, A. & Minh, B. Q. IQ-TREE: a fast and effective
568 stochastic algorithm for estimating maximum-likelihood phylogenies. *Mol. Biol. Evol.* **32**,
569 268–274 (2015).
570 66. Matschiner, M. Fitchi: haplotype genealogy graphs based on the Fitch algorithm.
571 *Bioinformatics* **32**, 1250–1252 (2016).
572 67. Excoffier, L. & Lischer, H. E. L. Arlequin suite ver 3.5: a new series of programs to perform
573 population genetics analyses under Linux and Windows. *Mol. Ecol. Resour.* **10**, 564–567
574 (2010).
575 68. Tajima, F. Statistical method for testing the neutral mutation hypothesis by DNA
576 polymorphism. *Genetics* **123**, 585–595 (1989).
577 69. Watterson, G. A. Heterosis or neutrality? *Genetics* **85**, 789–814 (1977).
578 70. Chakraborty, R. Mitochondrial DNA polymorphism reveals hidden heterogeneity within

579 some Asian populations. *Am. J. Hum. Genet.* **47**, 87–94 (1990).
580 71. Fu, Y. X. Statistical tests of neutrality of mutations against population growth, hitchhiking
581 and background selection. *Genetics* **147**, 915–925 (1997).
582 72. Korneliussen, T. S., Albrechtsen, A. & Nielsen, R. ANGSD: Analysis of next generation
583 sequencing data. *BMC Bioinformatics* **15**, 356 (2014).
584 73. Orlando, L. & Librado, P. Origin and evolution of deleterious mutations in horses. *Genes*
585 **10**, (2019).
586 74. Meisner, J. & Albrechtsen, A. Inferring population structure and admixture proportions in
587 low-depth NGS data. *Genetics* **210**, 719–731 (2018).
588 75. Skotte, L., Korneliussen, T. S. & Albrechtsen, A. Estimating individual admixture
589 proportions from next generation sequencing data. *Genetics* **195**, 693–702 (2013).
590 76. Lefort, V., Desper, R. & Gascuel, O. FastME 2.0: A comprehensive, accurate, and fast
591 distance-based phylogeny inference program. *Mol. Biol. Evol.* **32**, 2798–2800 (2015).
592 77. Pickrell, J. K. & Pritchard, J. K. Inference of population splits and mixtures from genome-
593 wide allele frequency data. *PLoS Genet.* **8**, e1002967 (2012).
594 78. Petkova, D., Novembre, J. & Stephens, M. Visualizing spatial population structure with
595 estimated effective migration surfaces. *Nat. Genet.* **48**, 94–100 (2016).
596 79. Mantel, N. The detection of disease clustering and a generalized regression approach.
597 *Cancer Res.* **27**, 209–220 (1967).
598 80. Lichstein, J. W. Multiple regression on distance matrices: a multivariate spatial analysis
599 tool. *Plant Ecol.* **188**, 117–131 (2007).
600 81. Slatkin, M. A measure of population subdivision based on microsatellite allele frequencies.
601 *Genetics* **139**, 457–462 (1995).
602 82. Pante, E., Simon-Bouhet, B. & Irisson, J.-O. *marmap - R package*. (2019).
603 83. Goslee, S. & Urban, D. The ecodist package for dissimilarity-based analysis of ecological
604 data. *Journal of Statistical Software, Articles* **22**, 1–19 (2007).

605 84. Soraggi, S., Wiuf, C. & Albrechtsen, A. Powerful inference with the D-statistic on low-
606 coverage whole-genome data. *G3* **8**, 551–566 (2018).

607
608

Acknowledgements

Financial support was provided by the Nansen Foundation and the Faculty of Mathematical and Natural Sciences, University of Oslo (UiO). We are grateful to the SEAPOP program (www.seapop.no/en, Norwegian Research Council grant number 192141), and the SEATRACK (http://www.seapop.no/en/seatrack) and ARCTOX (https://arctox.cnrs.fr/en/home) projects for collecting and sharing of samples. In particular, we thank Dave Fifield and Greg Robertson for the provision of puffin samples from Gull Island. The authors acknowledge support from the National Genomics Infrastructure in Stockholm funded by the Science for Life Laboratory, the Knut and Alice Wallenberg Foundation and the Swedish Research Council, and the SNIC/Uppsala Multidisciplinary Center for Advanced Computational Science for assistance with massively parallel sequencing (reference genome) and access to the UPPMAX computational infrastructure. Special thanks goes to the Norwegian Sequencing Centre (UiO) for the genomic libraries and resequencing of samples analyzed in this study. The razorbill genome data was made available for this study by Tom Gilbert and the Vertebrate Genome Project. Computation was performed using the resources and assistance from SIGMA2. Albína Pálsdóttir shared scripts for ANGSD, and Emiliano Trucchii advised on the manuscript. Pictures of puffins used in the figures were taken by Annemarie Look.

Author Contributions

SB and BS conceptualized the project. MI performed the DNA extraction for the reference genome. OK did all other laboratory work. KSJ advised on the sequencing strategy and co-supervised OK. OK refined the reference genome assembly. OK carried out the population genomic analyses with input from SB, BS and DML. OK designed the figures with input from SB, BS and DML. TAN, HS and ESH advised on colony selection and provided ecological context. TAN, HS, OdK, SD, ESH, JF, MPH, JD, KE, MLM and MGF provided samples. OK wrote the paper with SB, BS and DML. All authors read and revised the final version of the manuscript.

Competing Interests

The authors declare no competing interests.

Data availability

Raw read data have been deposited in the European Nucleotide Archive (ENA, www.ebi.ac.uk/ena) under study accession number PRJEB40631 (see Table S4 for individual sample accession numbers). Nuclear and mitochondrial scaffolds (GCA_905066775.1, CAJHIB010000001-CAJHIB010013329), as well as pseudo-chromosomes (GCA_905066775.2, CAJHIB020000001-CAJHIB020000027), have been uploaded to ENA (Project PRJEB40926, Sample SAMEA7482542).

Code availability

Full code used for the population genomic analyses is available on the first author's GitHub (https://github.com/OKersten/PuffPopGen).

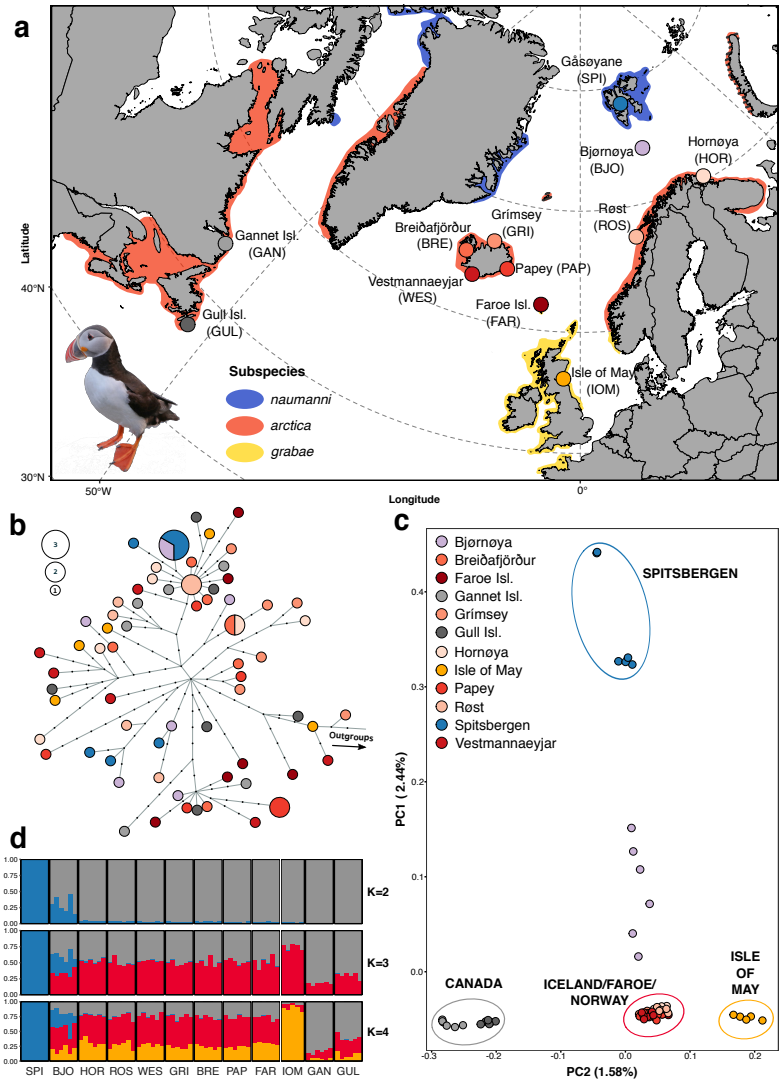

Figure 1: Sampling distribution and genomic structure of 71 Atlantic puffin individuals across 12 colonies throughout the breeding range. a) Map presenting the location of the 12 sampling sites. Colour shading indicates the breeding range of the species as a whole, as well as the recognized subspecies. b) Mitochondrial haplotype network constructed using the program Fitchi and a Maximum Likelihood tree generated in IQTree. It contains 66 unique haplotypes identified by 192 mitogenome-wide SNPs. Sizes of circles are proportional to haplotype abundance. Color legend is provided in c). Black dots represent inferred haplotypes that were not found in the present sampling. c) Principal Component Analysis (PCA) using genotype likelihoods at 1,093,765 polymorphic nuclear sites calculated in ANGSD to project the 71 individuals onto PC axes 1 and 2. Each circle represents a sample and colours indicate the different colonies. Percentage indicates proportion of genomic variation explained by each axis. The colour coding of the colonies is consistently used throughout the manuscript. d) CLUMPAK-averaged admixture plots of the best K's using the same genotype likelihood panel as in c). Each column represents a sample and colonies are separated by solid white lines. Optimal K's were determined by the method of Evanno et al. (2005) (see Figure S5a) and colors indicate the ancestry fraction to the different clusters.

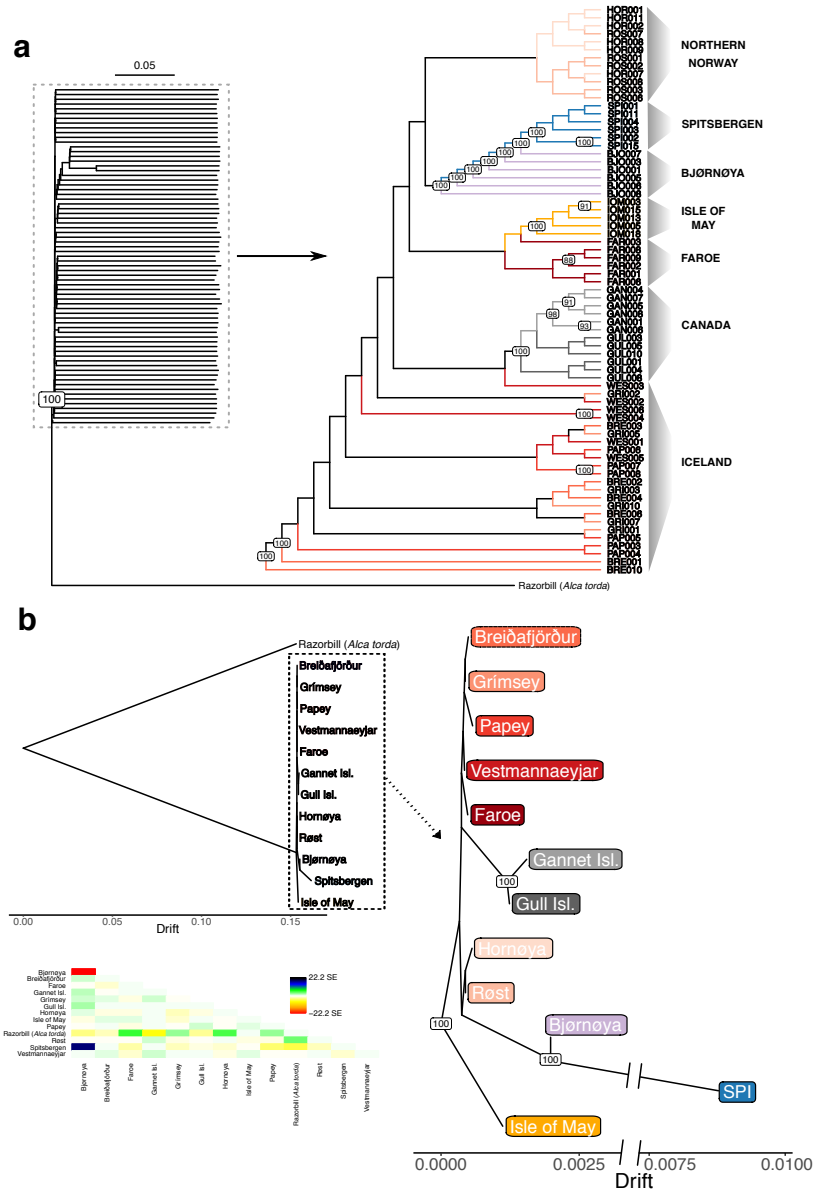

Figure 2: Phylogenetic reconstruction of individual and colony relationships from 71 Atlantic puffin individuals sampled across 12 colonies throughout the species' breeding range. a) An individual-based neighbor-joining tree constructed using pairwise p-distances calculated from genotype likelihoods at 1,093,765 polymorphic nuclear sites. Branch lengths and the outgroup were removed for the zoomed-in section to improve visualization. b) A population-based maximum likelihood Treemix analysis using allele frequencies at the same 1,093,765 polymorphic nuclear sites as in a). Both trees are rooted using the razorbill as an outgroup. The tree in b) is visualized with and without the outgroup. Branch lengths are equivalent to a genetic drift parameter. The heatmap indicates the residual fit of the tree displaying the standard error of the covariance between populations. In a) and b), the colour coding of the colonies is consistent with those in Figure 1 and node labels show bootstrap support >80.

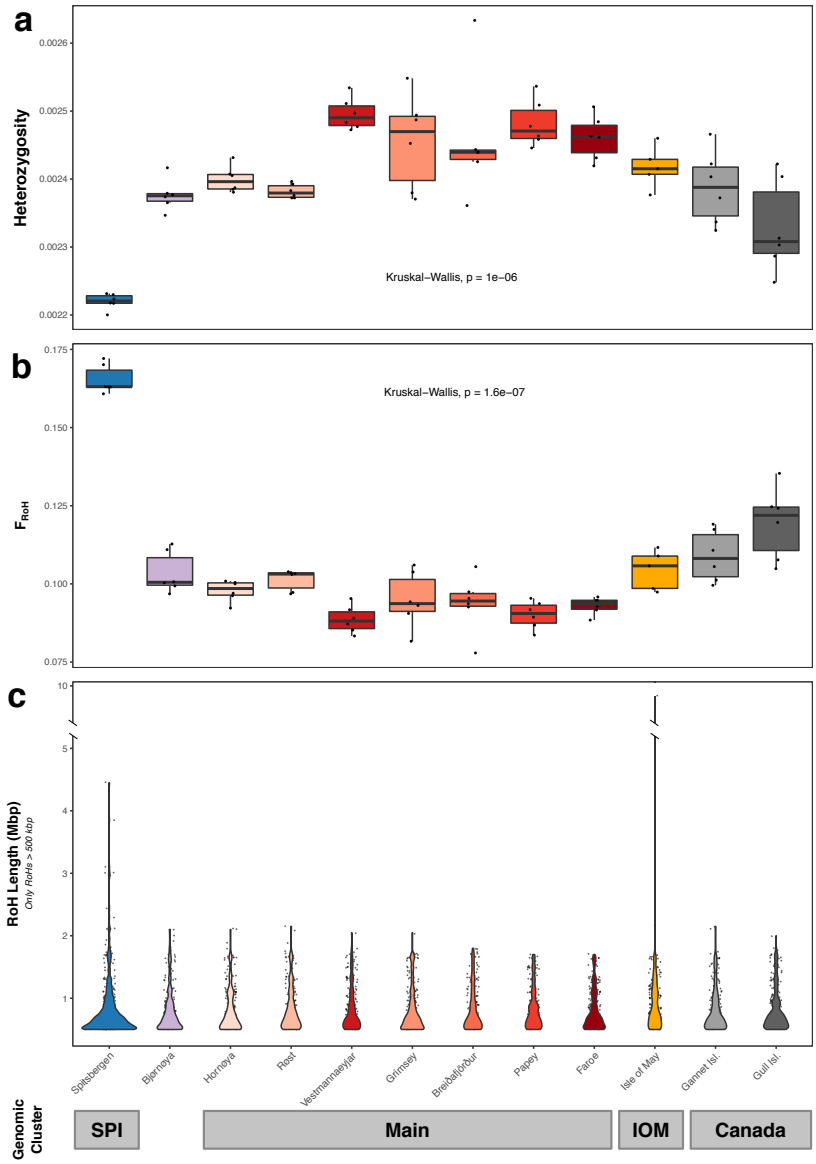

Figure 3: Genome-wide heterozygosity, inbreeding and Runs-of-Homozygosity (RoH) compared between 12 Atlantic puffin colonies across the species' breeding range. a) Estimates of individual genome-wide heterozygosity based on the per-sample one-dimensional Site Frequency Spectrum calculated in ANGSD. b) Individual inbreeding coefficients, F_{RoH}, defined as the fraction of the individual genomes falling into RoHs of a minimum length of 150 kbp. RoHs were declared as all regions with at least two subsequent 100 kbp windows harboring a heterozygosity below 1.435663 x 10^{-3}. c) RoH length distribution across the 12 colonies only including RoHs longer than 500 kbp. A single 9.65 Mbp long RoH on pseudo-chromosome 7 in an Isle of May individual required to introduce a break in the y-axis. In a) and b), black dots indicate individual sample estimates and black lines the median per colony, while in c), black dots represent single RoHs. Statistical significance of differences in heterozygosity and F_{RoH} between populations was assessed with a global Kruskal-Wallis test. The results of *post hoc* Dunn tests with Holm corrections are presented in Figure S11. Different colonies in all three plots are indicated using the same color code as in Figure 1.

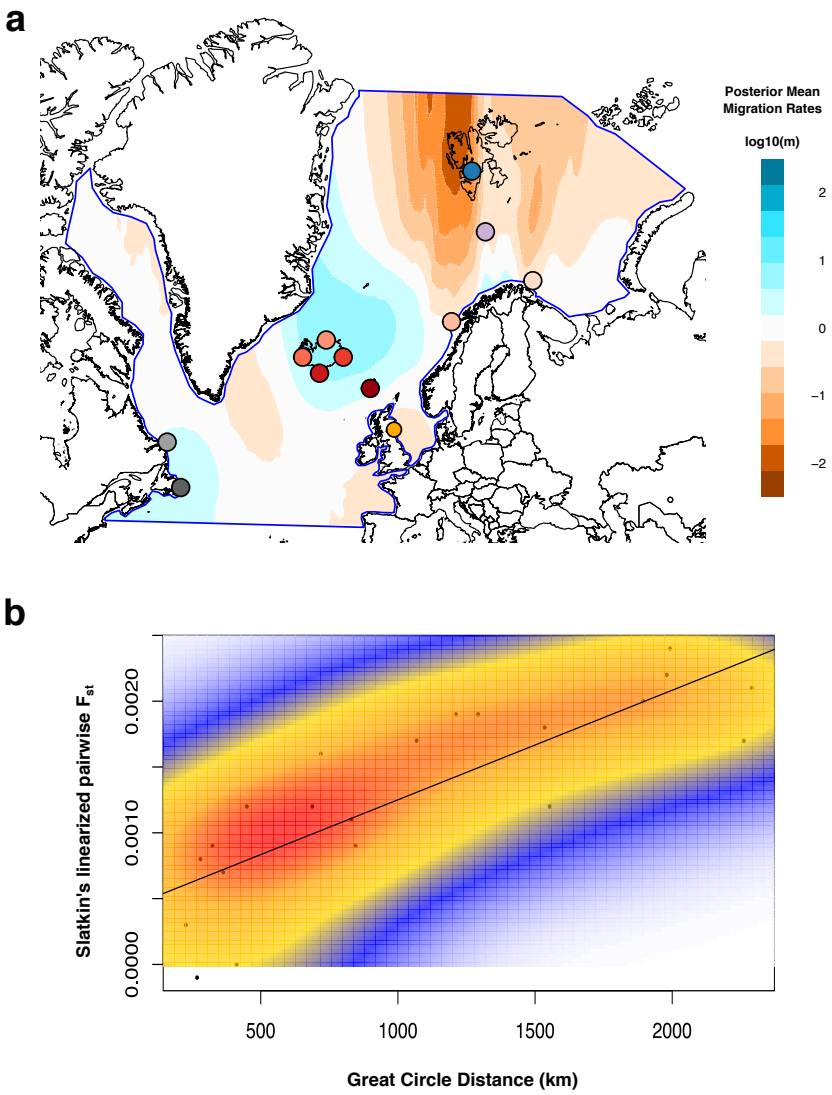

Figure 4: Estimates of continuous long-distance gene flow and isolation by distance (IBD) across the breeding range of the Atlantic puffin estimated from 71 individuals across 12 colonies. a) Effective migration surfaces inferred by the program EEMS using the average distance between pairs of individuals calculated in ANGSD by sampling the consensus base for each individual at 1,093,765 polymorphic nuclear sites. Darker reds indicate reduced migration across those areas, while darker blues highlight higher migration rates than the global mean. Different colonies are indicated using colors consistent with those in Figure 1. b) Correlation between genetic (Slatkin's linearized F_{ST}) and geographic (great-circle) distance presented after removing the Spitsbergen, Bjørnøya, Isle of May and Canadian individuals. The diagonal line visualizes the result of the Multiple Regression on Distance Matrices (MRM) analysis (slope and y-intercept). The Mantel test between genetic and geographic distance ($r = 0.826$, $p < 0.01$) was significant and 68.18% of variance in Slatkin's linearized F_{ST} was explained by geographic distance (regression coefficient of linear IBD model = 0.83×10^{-6}, $p < 0.01$). A two-dimensional kernel density estimation (kde2d) highlights dense groups of data points, thus substructure in the genomic landscape pattern. Analyses were conducted and results visualized in R using the *ecodist*, *marmap* and *MASS* packages.